Effect of Process Parameters on Selective Laser Melting Al_2O_3-Al Cermet Material

Hailong Liao*, Haihong Zhu*, Junjie Zhu†, Shijie Chang†, Xiaoyan Zeng*

*Wuhan National Laboratory for Optoelectronics, Huazhong University of Science and Technology, Wuhan, Hubei 430074, P. R. of China

†Shanghai Aerospace System Engineering Institute, Shanghai 201108, P.R. of China

Abstract

The cermet composite material is one of the researches focuses in the field of materials, for it can combine the toughness of metal and the hardness of ceramics. In this work, Al_2O_3-Al cermet composite with a mass ratio of 1:1 was fabricated by selective laser melting process. The effect of process parameters on the relative density and Al_2O_3 loss rate, as well as the Al_2O_3 loss mechanism, was investigated in detail. The results show that Al_2O_3 undergoes melt recrystallization and is significantly aggregated. The aggregated Al_2O_3 exhibits a network distribution in the metal matrix. The process parameters have a great influence on the relative density and the Al_2O_3 loss rate. As the scanning speed decreases, the relative density and the Al_2O_3 loss rate are changed with a contrary tendency. The loss mechanism is that the aluminum acts as a reducing agent, causing the Al_2O_3 becoming a gaseous substance Al_2O during selective laser melting process.

Introduction

Al_2O_3 ceramics have excellent wear resistance and corrosion resistance, which are rich in resources and low in price[1,2]. Therefore, the development and application of Al_2O_3 ceramic materials have a great economic effect. However, the brittleness of ceramics seriously restricts the development of their application[3]. Recently, the development of cermet material has made up for the lack of plasticity of Al_2O_3 ceramics. The cermet is composed of metal and ceramic, and the latter has a volume fraction of 15 to 85%[3].

Aluminum is one of the most widely used metals with high strength to weight ratio and low densities. It is also commonly used in the fabrication of cermet[4]. Al_2O_3-Al cermet materials have both excellent properties, such as high specific strength, high specific modulus, good wear resistance, etc[5,6]. They are promising in industry. Conventional methods for fabricating Al_2O_3-Al cermet materials generally include stir casting[7,8], hot isostatic pressing[9,10], and sintering[11,12]. However, these methods limit the application of Al_2O_3-Al cermet due to their inability to form part with complex structure. It is urgent to develop a new method for fabricating cermet part with complex structure.

Selective laser melting (SLM) is now widely used in the aerospace industry because of its ability to form complex shaped parts[13–15]. Studies have shown that this method can also be applied to the manufacture of cermet materials[16,17]. This paper investigates the effect of process parameters on the selective laser melting of Al_2O_3-Al cermet with a mass fraction of 50wt%.

Materials and experiment procedures

Materials and SLM process

The polygonal Al_2O_3 powder used in this experiment has an average particle size of 26.6 μm. The aluminium alloy powder is the AlSi10Mg with an average particle size of 33.1μm. Ball milling was performed in a tumbling ball mill to obtain uniform Al_2O_3-AlSi10Mg composite powder, according to the weight ratio of

1:1(Fig.1). It reveals that the morphology and dispersion state of the mixed Al_2O_3-AlSi10Mg powders do not change markedly under the condition of mechanical blending.
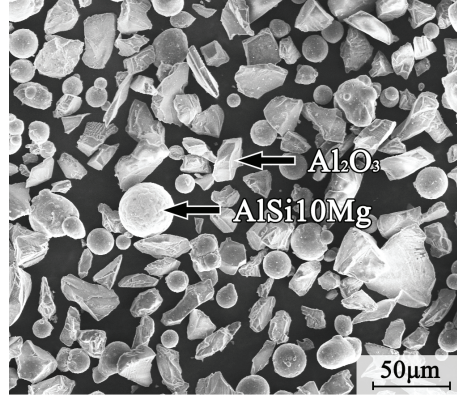

Fig.1. SEM image of the mixed Al_2O_3-AlSi10Mg composite powders after ball milling

The experiments were carried out on a self-developed SLM-100 machine that equipped with an IPG YLR-200 fiber laser (λ=1.07μm) with a maximum output power of 200W, an automatic powder layering appliance and an inert argon gas protection system. The SLM machine was described in detail in our previous publication[18]. The specimens were to be prepared on an AA 2024 aluminum alloy substrate with dimensions of 140mm×140mm×35mm. The process was carried out under argon atmosphere with the concentration of O_2 controlled below 200ppm.

The sample with a size of 5mm×5mm×5mm was preliminarily fabricated using several parameters sets in order to study the effect of processing parameter. The used detailed parameters are shown in Table 1.

Table 1
Processing parameters used in this study.

Manufacturing parameters	Value
Laser power P, W	200
Scanning speed v, m/s	150,200,250,300 and 350
Layer thickness t, μm	20
Hatching space h, mm	0.05, 0.10

Characterization

The relative density and Al_2O_3 loss rate of the samples were evaluated by an image process algorithm (IPA) based on C# language. This method was described in detail in our previous study[17]. The Al_2O_3 loss rate (S) is determined by Eq. (1):

$$S = \frac{M_0 - M_1}{M_0} \times 100\%$$

(1)

where M_0 is the mass fraction of Al_2O_3 in the starting mixed powder, M_1 is the mass fraction of Al_2O_3 in the SLMed sample. The M_1 can be calculated as Eq. (2):

$$M_1 = \frac{V_1 \times \rho_{Al_2O_3}}{V_1 \times \rho_{Al_2O_3} + (1 - V_1) \times \rho_{Al}}$$

(2)

where $\rho_{Al_2O_3}$ and ρ_{Al} are the theoretical densities of Al_2O_3 and Al, respectively. V_1 is the area fraction of Al_2O_3, which can be determined by IPA[17]. The laser energy density is defined as Eq. (3).

$$E_d = \frac{P}{vh\delta}$$

(3)

where E_d is the laser energy density in J/mm^3, v is the scanning speed (mm/s), h is the hatching space, δ is the layer thickness.

The metallographic samples were prepared according to the standard procedures and then etched by a solvent composed of 95 ml water, 2.5 ml HNO_3, 1.5 ml HCl and 1.0 ml HF (every 100 ml solution). The

microstructure was characterized using the scanning electron microscopy (SEM, FEI Nova NanoSEM 450) equipped with an energy dispersive spectrometry (EDS, Oxford X-Max 50) microprobe system and optical microscopy (OM, Nikon EPIPHOT). Phase identification was performed by X-ray diffraction (XRD) using a PANalytical X´pert PRO with Cu Kα radiation. On all averaged values, a confidence interval of 95%, based on the variance σ_{n-1}, is used to indicate the spread.

Results and discussions

Microstructure

Fig.2 shows the SEM image of the vertical cross of SLMed sample fabricated under the speed of 350mm/s and hatching space of 0.10mm. The white substance is Al_2O_3. It is apparent that the Al_2O_3 undergoes melting and recrystallization. The molten Al_2O_3 aggregates in the molten pool and exhibits a network distribution. The red arrow identifies the unfused pore near the Al_2O_3 in Fig.2a. As an additive, Al_2O_3 affects the flow of AlSi10Mg in the molten pool, especially the molten Al_2O_3, which easily hinders the flow of the molten pool. Thereby, unfused pores are formed. As shown in Fig. 2b, the aggregated Al_2O_3 ceramics have microcracks. It can be seen that the ceramic still exhibits strong brittleness. Of course, this is also related to the SLM being a fast cooling rate and high-temperature gradient. Al_2O_3 is prone to form micro-cracks during the process.

Fig.3 is a photomicrograph of SLMed sample under different process parameters. The process parameters have a great influence on the distribution state of Al_2O_3. When the hatching space is 0.05 mm and scanning speed is 150mm/s, Al_2O_3 exhibits local aggregation, as shown by the white area in Fig. 3a-1. As the scanning speed increases, the Al_2O_3 distribution is more uniform and the content of Al_2O_3 in the matrix increases. When the hatching space is 0.10mm, the Al_2O_3 exhibits a network distribution, especially when the scanning speed is greater than 250 mm/s.

Fig.4 is the XRD diffraction pattern of the typical SLM formed Al_2O_3-AlSi10Mg composite. The XRD results show that the diffraction peak of Al_2O_3 decreases with the increase of the energy density. This confirms the occurrence of Al_2O_3 loss. As the energy density increases, i.e. the hatching space or scanning speed decreases, the Al_2O_3 loss increases significantly, as shown in Fig.3a-1 and Fig.3b-5. A uniform distribution of Al_2O_3-AlSi10Mg composites is obtained when scanning speed is in the range of 250 mm/s to 350 mm/s and the hatching space is 0.10mm.
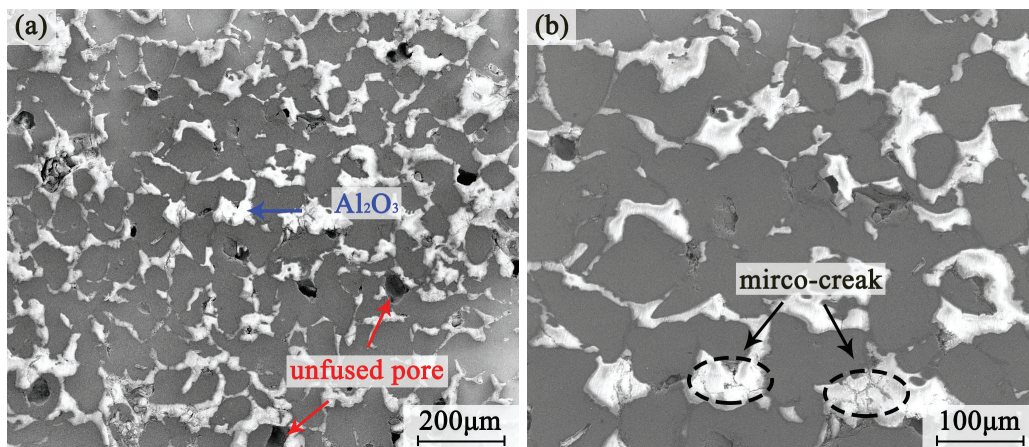

Fig.2. SEM image of the vertical cross of SLMed sample fabricated under the scanning speed of 350mm/s and hatching space of 0.10mm
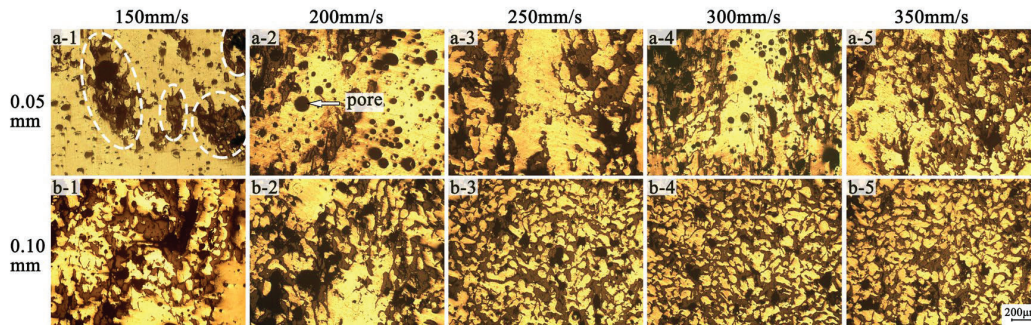
Fig.3. Polished cross-sections of SLM-fabricated Al_2O_3-AlSi10Mg sample under varying process parameters

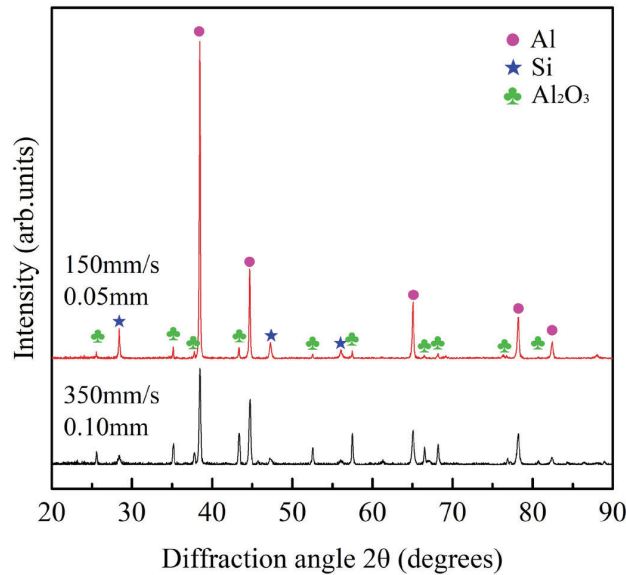**Relative density and Al_2O_3 loss**

Fig.5 shows the relative density of SLMed samples at different scanning speeds. As the scanning speed increases, the relative density slowly increases. When the hatching space is 0.10mm and the scanning speed is 250mm/s, the highest relative density can be achieved to 94%. When the scanning speed is greater than 250mm/s, higher than 93% relative density also can be achieved. This is because at low scanning speed, the energy density is high and a large number of pores appear. The pores are formed at low scanning speeds from gases trapped within the molten pool or evolved from the powder during solidification[19]. The distribution of Al_2O_3 is also more uniform as the scanning speed increases as shown in Fig.3, which reduces the possibility of defects. Noteworthy that as the scanning speed continues to increase, the relative density may decrease.
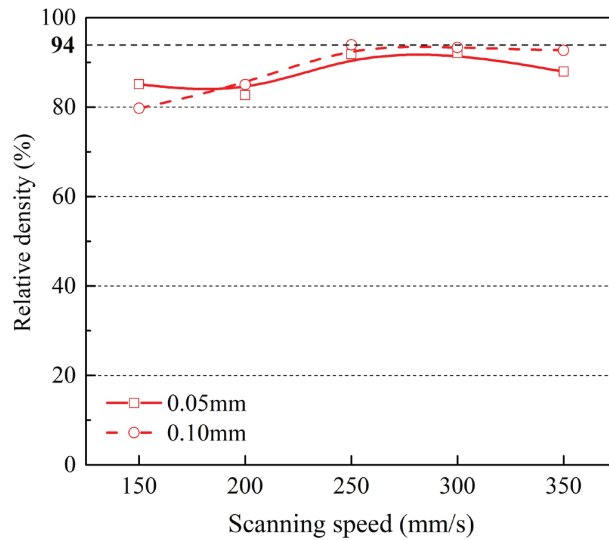
Fig.5. The relative density under varying scanning speed and hatching space

Fig.6 shows the variation of Al_2O_3 loss rate with the scanning speed at different hatching space. Apparently that the relative density and the Al_2O_3 loss rate show a contrary tendency. As the scanning speed and hatching space increase, the loss rate of Al_2O_3 gradually decreases. When the hatching space is 0.10mm and the scanning speed is higher than 250 mm/s, the Al_2O_3 loss rate is less than 7.6%. It has been confirmed that Al_2O_3 and aluminum undergo redox reactions under high temperature conditions. Al_2O_3 is easily reduced by aluminum to form Al_2O gas and overflows the molten pool[17].
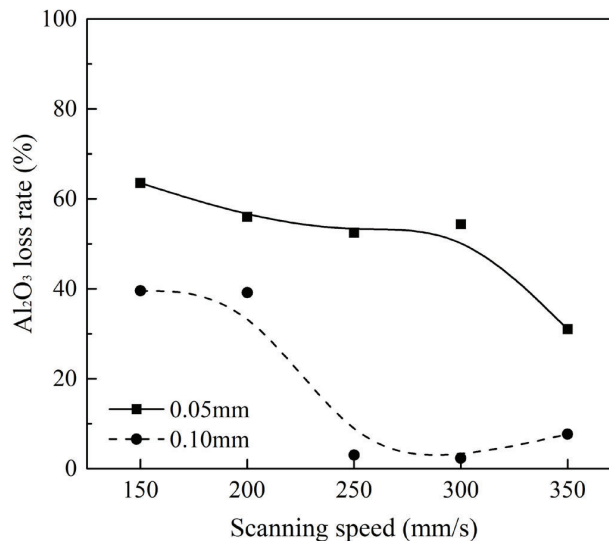

Fig.6. The Al_2O_3 loss rate under varying scanning speed and hatching space

Conclusions

The microstructure of SLMed Al_2O_3-AlSi10Mg cermet material with a mass ratio of 1:1 were investigated. The Al_2O_3 ceramic in Al_2O_3-AlSi10Mg undergoes melting recrystallization under laser irradiation. When the hatching space is 0.05 mm, the Al_2O_3 tends to locally aggregate. As the scanning speed or hatching space increases, the Al_2O_3 gradually disperses and exhibits a network distribution. The effect of process parameters on the relative density and Al_2O_3 loss rate was also studied. The relative density and the Al_2O_3 loss show with a contrary tendency. As the hatching spacing or scanning speed increases, the density increases and the Al_2O_3 loss decreases. The Al_2O_3 loss is caused by the reduction of the aluminum alloy at high temperature to form Al_2O gas.

Future works

As that process parameters affect the loss and distribution of Al_2O_3. Future work will focus on how to avoid loss and agglomeration of Al_2O_3. And the optimized process parameters will be obtained after doing more experiments and analysis.

Acknowledgements

References

[1] Y. Dianran, H. Jining, W. Jianjun, Q. Wanqi, M. Jing, The corrosion behaviour of a plasma spraying Al2O3 , ceramic coating in dilute HC1 solution, 89 (1997) 191–195.

[2] M. Hazra, A.K. Mondal, S. Kumar, C. Blawert, N.B. Dahotre, Laser surface cladding of MRI 153M magnesium alloy with (Al+Al2O3), Surf. Coatings Technol. 203 (2009) 2292–2299.

[3] R. Wang, X. Wang, S. Dong, N. Niu, D. Chang, C. Yu, J. Song, S. Li, Effect of Molding Pressure on Densification of Al2O3 / Al Cermet Materials, 893 (2017) 100–104.

[4] A. Heidarpour, S. Ahmadifard, S. Kazemi, Fabrication and Characterization of Al5083 / Al 2 O 3 Surface Nanocomposite via Friction Stir Processing, 5 (2017) 11–24.

[5] D.B. Miracle, Metal matrix composites - From science to technological significance, Compos. Sci. Technol. 65 (2005) 2526–2540.

[6] J. Jue, D. Gu, K. Chang, D. Dai, Microstructure evolution and mechanical properties of Al-Al2O3composites fabricated by selective laser melting, Powder Technol. 310 (2017) 80–91.

[7] A. Kumar, S. Lal, S. Kumar, Fabrication and characterization of A359 / Al 2 O 3 metal matrix composite using electromagnetic stir casting method, Integr. Med. Res. 2 (2013) 250–254.

[8] M. Kok, Production and mechanical properties of Al2O3 particle-reinforced 2024 aluminium alloy composites, J. Mater. Process. Technol. 161 (2005) 381–387.

[9] A.M.A. Mohamed, M. Gupta, Effect of reinforcement concentration on the properties of hot extruded Al-Al2O3 composites synthesized through microwave sintering process, Mater. Sci. Eng. A. 696 (2017) 60–69.

[10] A.M. Al-Qutub, I.M. Allam, M.A. Abdul Samad, Wear and friction of Al–Al2O3 composites at various sliding speeds, J. Mater. Sci. 43 (2008) 5797–5803.

[11] M. Rahimian, N. Ehsani, N. Parvin, H.R. Baharvandi, The effect of sintering temperature and the amount of reinforcement on the properties of Al-Al2O3 composite, Mater. Des. 30 (2009) 3333–3337.

[12] A.N. Abed, B.A. Sabri, Microstructure and Density Characterization for Nano and Micro Al_2O_3-Aluminum Composites Produced by Powder Metallurgy Process Experimental procedures :, 20 (2017) 1024–1033.

[13] H. Zhang, H. Zhu, X. Nie, J. Yin, Z. Hu, X. Zeng, Effect of Zirconium addition on crack, microstructure and mechanical behavior of selective laser melted Al-Cu-Mg alloy, Scr. Mater. 134 (2017) 6–10.

[14] S. Zhang, H. Zhu, Z. Hu, X. Zeng, F. Zhong, Selective Laser Melting of Cu-10Zn alloy powder using high laser power, Powder Technol. 342 (2019) 613–620.

[15] J. Jue, D. Gu, Selective laser melting additive manufacturing of in situ Al 2 Si 4 O 10 /Al composites: Microstructural characteristics and mechanical properties, J. Compos. Mater. 51 (2017) 519–532.

[16] Q. Han, Y. Geng, R. Setchi, F. Lacan, D. Gu, S.L. Evans, J. Jue, D. Gu, K. Chang, D. Dai, Q. Han, R. Setchi, F. Lacan, D. Gu, S.L. Evans, Microstructure evolution and mechanical properties of Al-Al2O3composites fabricated by selective laser melting, Powder Technol. 127 (2017) 26–35.

[17]   H. Liao, H. Zhu, G. Xue, X. Zeng, Al_2O_3 loss mechanism of Al 2 O 3 -AlSi10 Mg composites during selective laser melting, J. Alloys Compd. 785 (2019) 286–295.

[18]   Z. Wang, K. Guan, M. Gao, X. Li, X. Chen, X. Zeng, The microstructure and mechanical properties of deposited-IN718 by selective laser melting, J. Alloys Compd. 513 (2012) 518–523.

[19]   N.T. Aboulkhair, N.M. Everitt, I. Ashcroft, C. Tuck, Reducing porosity in AlSi10Mg parts processed by selective laser melting, Addit. Manuf. 1 (2014) 77–86.